

Article

# Investigating the Effect of Uncertainty Characteristics of Renewable Energy Resources on Power System Flexibility

Changgi Min

Department of Electrical and Electronic Engineering, Joongbu University, 305 Dongheon-ro, Deogyang-gu, Goyang-si, Gyeonggi-do 10279, Korea; cgmin@joongbu.ac.kr; Tel.: +82-31-8075-1635

**Featured Application:** This study proposes a method for quantifying the effect of uncertainty characteristics of renewable energy resources on power system flexibility, based on the ramping capability shortage probability index. The procedure involves scenario generation and evaluation of uncertainty characteristics. The proposed approach can provide system operators with the means to evaluate uncertainty characteristics, as well as possible strategies for a more flexible power system.

**Abstract:** This study investigates the effect of uncertainty characteristics of renewable energy resources on the flexibility of a power system. The more renewable energy resources introduced, the greater the imbalance between load and generation. Securing the flexibility of the system is becoming important to manage this situation. The degree of flexibility cannot be independent of the uncertainty of the power system. However, most existing studies on flexibility have not explicitly considered the effects of uncertainty characteristics. Therefore, this study proposes a method to quantitatively analyze the effect of uncertainty characteristics on power system flexibility. Here, the uncertainties of the power system indicate the net load forecast error, which can be represented as a probability distribution. Of the characteristics of the net load forecast error, skewness and kurtosis were considered. The net load forecast error was modeled with a Pearson distribution, which has been widely used to generate the probability density function with skewness and kurtosis. Scenarios for the forecast net load, skewness, and kurtosis were generated, and their effects on flexibility were evaluated. The simulation results for the scenarios based on a modified IEEE-RTS-96 revealed that skewness is more effective than kurtosis. The proposed method can help system operators to efficiently respond to changes in the uncertainty characteristics of renewable energy resources.



**Citation:** Min, C. Investigating the Effect of Uncertainty Characteristics of Renewable Energy Resources on Power System Flexibility. *Appl. Sci.* **2021**, *11*, 5381. <https://doi.org/10.3390/app11125381>

Academic Editor: Radu Godina

Received: 9 May 2021

Accepted: 8 June 2021

Published: 10 June 2021

**Publisher's Note:** MDPI stays neutral with regard to jurisdictional claims in published maps and institutional affiliations.



**Copyright:** © 2021 by the author. Licensee MDPI, Basel, Switzerland. This article is an open access article distributed under the terms and conditions of the Creative Commons Attribution (CC BY) license (<https://creativecommons.org/licenses/by/4.0/>).

**Keywords:** flexibility; kurtosis; ramping capability shortage probability (RSP); renewable energy resource (RER); skewness; uncertainty; Pearson distribution

## 1. Introduction

Since the adoption of the Paris Agreement in 2015, global CO<sub>2</sub> emissions have risen by approximately 4% [1]. In the future, energy transition and proactive efforts such as revising the nationally determined contributions in each country are needed to reduce emissions. The Korean government has been struggling with the enactment and reformation of policies and systems related to climate change and energy transition. The Energy Transition Roadmap and the Renewable Energy 3020 Implementation Plan were established in 2017 [2,3], and many efforts have been made since then to reduce coal power plants and expand new and renewable energy resources. In the Ninth Basic Electric Power Supply and Demand Plan established in 2020, the ratio of renewable energy generation to the total electricity generation in 2040 is targeted at 26.3% (for reference, its value in 2020 was 7.5%) [4]. To enhance the realizability of this plan and revitalize the related industrial ecosystems under these plans, the Fifth Renewable Energy Basic Plan was established in 2020 [5].

Along with these policy and institutional efforts, one of the essentials in introducing massive renewable energy resources (RERs) is to enhance the flexibility of power systems, although comprehensive strategies considering the energy sector coupled with using technologies such as power to gas (P2G) and power to heat (P2H) equally count [6]. The large penetration of RER into the power system is likely to increase the volatility and uncertainty of the net load, i.e., the load minus the output of the RER [7]. A growing amount of variable generation, such as wind and photovoltaic (PV) power plants, requires more flexibility, where flexibility is defined as the ability of a power system to respond to the change in net load [8]. The flexibility issue indicates a situation associated with a lack of flexibility [9,10]. System operators have begun to confront this problem and make various efforts to enhance adequate flexibility. It is related to not only improving the related infrastructure and system, such as the development of market mechanisms for flexibly supplying resources and preemptive network reinforcement, but also advancing the RER output forecasting technique and the flexibility-considered operation [11,12].

The uncertainty of the RER may largely affect the flexibility of the power system, as it relates to the shortage risk of flexibility. The uncertainty of the RER in the power system indicates the forecast error of the RER output, which may cause an unserved net load. Irrespective of how well the RER output is predicted, its forecast error is inevitable. Thus, the system operator should consider the forecast error when determining an adequate level of flexibility [13]. The RER forecast error has been modeled using various types of probability distributions, such as normal [14–16], Weibull [17], Rayleigh [18], and beta [19] distributions. In most studies on flexibility evaluation, the RER forecast error has often been assumed to follow a normal distribution, which has a limit in reflecting the characteristics of actual error distributions [20,21]. Skewness and kurtosis are representative characteristics of error distribution [22]. If these characteristics are neglected in the flexibility evaluation, the system operator may underestimate or overestimate the shortage risk of flexibility and accordingly may not be able to respond to the net load variation. Although normal distribution [23,24] and conditional distributions based on historical data [25] have been used in existing research on flexibility evaluation, the effect of the characteristics of the forecast error on flexibility is yet to be explicitly analyzed.

This study investigates the effect of changes in the uncertainty characteristics of the RER on the flexibility of a power system. An index called the ramping capability shortage probability (RSP) is used to assess flexibility [26]. The Pearson distribution is applied to model a probability density function (PDF) with the characteristics of skewness and kurtosis. The scenarios for evaluation were generated by changing three parameters—forecast net load (FNL), skewness, and kurtosis. An analysis procedure for the impact of the uncertainty characteristics on flexibility is proposed. Through the simulation results for the scenarios, a more effective parameter was confirmed.

The remainder of this paper is organized as follows: Section 2 introduces the flexibility index RSP, which can quantify the flexibility. Section 3 explains the modeling of NLFE using the Pearson distribution and describes the analysis procedure for the impact of NLFE on flexibility. In Section 4, a scenario-based simulation for a modified IEEE-RTS-96 is presented. The conclusions and future work are presented in Section 5.

## 2. Flexibility Index: Ramping Capability Shortage Probability

The effect of uncertainty on flexibility can be quantified using a flexibility index called RSP. It is useful for power-system operators to manage the flexibility shortage situation. The details of the RSP are as follows.

### 2.1. System Ramping Capability (SRC), Ramping Capability Requirement (RCR)

The ramping capability (RC) of a power generation unit is defined as the ability to change in a power generation of a unit over a given period. The aggregated RC can be thought of as the system's ability to respond to load-generated imbalance due to

uncertainties. Flexibility relies on the secured RC. The system RC (*SRC*) is the total RC in the system and can be formulated as:

$$SRC_t = \sum_{i \in I} A_{i,t-\Delta t} O_{i,t-\Delta t} \min(P_{max,i} - P_{i,t-\Delta t}, rr_i \Delta t) \tag{1}$$

Here, *I* means a set of generators.  $A_{i,t-\Delta t}$  is a random variable representing the availability of generator *i* at time  $t-\Delta t$ .  $O_{i,t-\Delta t}$  is a variable representing whether generator *i* is online at time  $t-\Delta t$ .  $\min()$  is a function selecting a smaller value in the brackets.  $P_{max,i}$  is a maximum output of generator *i*.  $P_{i,t-\Delta t}$  is the output of generator *i* at time  $t-\Delta t$ .  $Rr_i$  is the ramp rate of generator *i*.  $\Delta t$  is the minimum interval between operating points. The  $SRC_t$  represents the amount of RC the system can supply during time  $\Delta t$ , considering the uncertainty. The larger the *SRC*, the greater the flexibility. However, the uncertainty of the system can reduce the RC availability, which directly relates to the parameter  $A_{i,t-\Delta t}$ , which indicates whether the unit fails from  $t-\Delta t$  to  $t$ . The values of  $O_{i,t-\Delta t}$  and  $P_{i,t-\Delta t}$  are determined by the generation schedule.

The RC requirement (*RCR*) can be expressed as follows:

$$RCR_t = NLFE_t + FNL_t - \sum_{i \in I} A_{i,t-\Delta t} O_{i,t-\Delta t} P_{i,t-\Delta t} \tag{2}$$

where

$$NLFE_t = LFE_t - VGFE_t \tag{3}$$

$$FNL_t = FL_t - FVG_t \tag{4}$$

Here,  $NLFE_t$  is a random variable representing net load forecast error at time  $t$ .  $FNL_t$  is a forecast net load at time  $t$ .  $LFE_t$  is a random variable representing load-forecast error at time  $t$ .  $VGFE_t$  is a random variable representing variable generation forecast error at time  $t$ .  $FL_t$  is a forecasted load at time  $t$ .  $FVG_t$  is the forecast variable generation at time  $t$ . The  $RCR_t$  indicates the amount of RC required to manage unexpected net load fluctuations and unit failures from  $t-\Delta t$  to  $t$ . The random variables  $NLFE_t$ ,  $LFE_t$ , and  $VGFE_t$  represent the forecast errors.

### 2.2. Ramping Capability Shortage Probability (RSP)

If the situation where  $SRC_t$  is lower than  $RCR_t$  continues, load shedding is required; this situation is called the RC shortage. The risk of an RC shortage at time  $t$  is defined as the RC shortage probability ( $RSP_t$ ) and is represented as follows:

$$RSP_t = \sum_{e \in E_t} Prob(e) \left[ \sum_{c \in C_{t-\Delta t}} Prob_c \left[ FNL_t + NLFE_t > \sum_{i \in I} A_{i,t-\Delta t} O_{i,t-\Delta t} \{P_{i,t-\Delta t} + \min(P_{max,i} - P_{i,t-\Delta t}, rr_i \Delta t)\} \right] \right] \tag{5}$$

Here,  $E_t$  is a set of  $NLFE_t$  and  $e$  is an element of  $E_t$ .  $Prob(\cdot)$  is a function calculating probability in the brackets.  $C_{t-\Delta t}$  is a set of combinations of  $A_{i,t-\Delta t}$  when  $O_{i,t-\Delta t}$  is nonzero for all  $i$ .  $c$  is an element of  $C_{t-\Delta t}$ .  $Prob_c[\cdot]$  means a probability of  $c$  if condition  $[\cdot]$  is satisfied, 0 otherwise. The random variables representing the uncertainties are  $A_{i,t-\Delta t}$  and  $NLFE_t$ .  $C_{t-\Delta t}$  and  $E_t$  are the set of possible cases for  $A_{i,t-\Delta t}$  and  $NLFE_t$ , respectively.  $FNL_t$  determines an online set of generating units, and  $NLFE_t$  is expressed as the % value of  $FNL_t$ ; thus, any variation in  $FNL_t$  may affect not only  $O_{i,t-\Delta t}$  and  $P_{i,t-\Delta t}$  but also  $A_{i,t-\Delta t}$  and  $NLFE_t$ . The  $RSP_t$  is calculated in the worst-case scenario, i.e., unexpected unit failures and net-load deviation occur just before the considered time  $t$ , and the imbalance cannot be resolved by a post-recovery action. This consideration is useful for reducing the computational burden of large-scale power systems. Meanwhile, the effect of complementarity between RERs is reflected in the  $NLFE_t$ . If the aggregated output of RERs changes,  $FNL_t$  varies, and  $VGFE_t$  and  $NLFE_t$  vary accordingly. For reference,  $C_{t-\Delta t}$  is exemplified as follows: two generating units are online at times 1 and 2. The state of each unit at each time can be represented as either 1 (online) or 0 (failed). All possible cases at time 1 (i.e.,  $C_1$ ) are thus

represented as (0,0), (0,1), (1,0), and (1,1). For reference, the probability of every element is calculated using a Markov-chain-based generator model; for further details, please refer to [27].  $E_t$  is exemplified as follows:  $FNL_t$  at time  $t$  is 10 MW. The  $NLFE_t$  is assumed to follow the skewed distribution shown in Figure 1.  $E_t$  is thus (−1 MW), (0 MW), and (1 MW) by multiplying 10% and 10 MW, and the probability of each element is 0.25, 0.25, and 0.5, respectively.

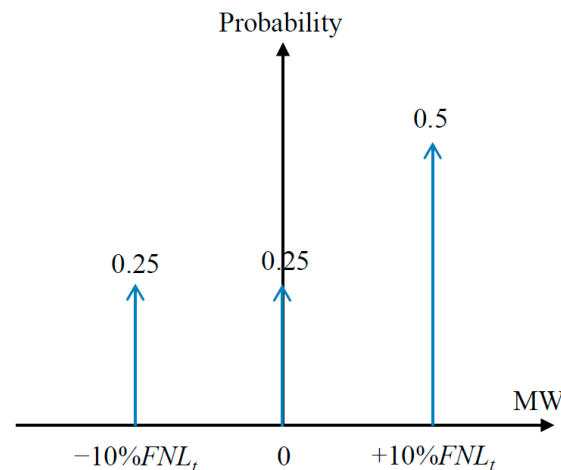


**Figure 1.** Probability distribution for  $E_t$ .

### 3. Evaluation of the Effect of Uncertainty Characteristics on Flexibility

#### 3.1. Modeling NLFE Characteristics Using a Pearson Distribution

The output of RERs is volatile and uncertain. The forecasted output involves a forecast error, which can be modeled as a random variable. Regardless of how well the output is predicted, the forecast error is inevitable, and the system operator cannot avoid it. Flexibility enhancement is thus necessary to deal with the forecast error, which indicates the risk of the system. The system operator should determine an adequate level of flexibility, which can be quantified using the RSP index. The forecast error of the renewable energy resource, i.e., VGFE, is reflected within the NLFE in the RSP calculation, i.e., NLFE is set as LFE minus VGFE. This RSP method was used to estimate the RC shortage, and the RC requirement was associated with the NLFE.

The normal distribution has been used to model NLFE in the RSP calculation [28,29]; however, it has a limitation in representing the distribution of NLFE characteristics such as skewness and kurtosis [30]. The Pearson distribution has been widely used to generate the PDF with skewness and kurtosis [31]. An advantage of the Pearson distribution over other distributions, such as the Weibull distribution, is the use of PDF moments to determine the distribution parameters. This distribution can be modeled as a function of skewness and kurtosis, and it allows the separate analysis of the effects of skewness and kurtosis. Thus, the Pearson distribution is applied to the NLFE model. It refers to a family of several probability distributions; it is made up of seven probability distributions, i.e., Type I to VII. If the values of the first four moments are known, i.e., mean, standard deviation, skewness, and kurtosis, the PDFs can be generated. Some of these types are listed in Table 1.

**Table 1.** Main PDF types of the Pearson distribution according to the parameter  $\gamma$ .

PDF Type	Equations with Origin at the Mean	Type Decision
I	$\phi^*(z^*) = y_0(1+z^*/A_1)^{m_1}(1-z^*/A_2)^{m_2}$	$-\infty < \gamma < 0$
IV	$\phi^*(z^*) = y_0 \left(1 + (z^*/a - v/r)^2\right)^{-m} e^{-v \tan^{-1}(z^*/a - v/r)}$	$0 < \gamma < 1$
VI	$\phi^*(z^*) = y_0(1+z^*/A_1)^{-q_1}(1+z^*/A_2)^{q_2}$	$1 < \gamma < \infty$
Normal Curve	$\phi^*(z^*) = \frac{1}{\sqrt{2\pi}} e^{-(z^{*2}/2)}$	$\gamma = 0, P_{sk} = 0, P_k = 0$
II	$\phi^*(z^*) = y_0(1-z^{*2}/a^2)^m$	$\gamma = 0, P_{sk} = 0, P_k < 3$
VII	$\phi^*(z^*) = y_0(1+z^{*2}/a^2)^{-m}$	$\gamma = 0, P_{sk} = 0, P_k > 3$

In the last column, the parameter  $\gamma$  is defined as follows:

$$\gamma = \frac{P_{sk}^2(P_k + 3)^2}{4(2P_k - 3P_{sk}^2 - 6)(4P_k - 3P_{sk}^2)} \tag{6}$$

where  $P_{sk}$  and  $P_k$  are the skewness and kurtosis of the NLFE, respectively. The PDF type is determined according to  $P_{sk}, P_k$ , and  $\gamma$ . For reference, parameters such as  $y_0, A_1, A_2, m_1, m_2, a, r, v, m, q_1$ , and  $q_2$  can be calculated using the following moments: mean, standard deviation, skewness ( $P_s$ ), and kurtosis ( $P_k$ ). For further details, please refer to [32]. Table 2 presents a simple example of the parameters of the Pearson distribution of NLFE, and the corresponding results are shown in Figure 1. The skewness and kurtosis are only varied, i.e., the mean and standard deviations are kept the same. The results for C11 to C17 and those of C21 to C27 correspond to Figure 2a,b, respectively.

In Figure 2a, the PDF for the negative (positive) skewness is skewed to the left (right). In Figure 2b, the larger the kurtosis, the sharper the PDF at the center; however, the difference between each PDF according to the increase in kurtosis becomes increasingly smaller.

**Table 2.** Numerical example of Pearson distribution of NLFE: (mean: 0, standard deviation: 1).

Case	Skewness	Kurtosis	PDF Type
C11	0	3	0
C12	-0.3	3	1
C13	-0.5	3	1
C14	-0.7	3	1
C15	0.3	3	1
C16	0.5	3	1
C17	0.7	3	1
C21	0	4	7
C22	0	5	7
C23	0	6	7
C24	0	8	7
C25	0	10	7
C26	0	50	7
C27	0	200	7

### 3.2. Evaluation Procedure for the Effect of NLFE Characteristics on Flexibility

To define the effect-evaluation procedure, the following thing was first considered: the time interval when the largest  $RSP_t$  occurs was chosen because it is the riskiest time in terms of flexibility. This assumption helps enhance analyzability while considering that the entire time interval may be time-consuming in analyzing the result. Moreover, this study does not focus on evaluating the flexibility related to the load-generation balance for the whole period but rather on analyzing the effect on flexibility according to the changes in the NLFE characteristics. If the entire period is considered, the effect of the NLFE characteristics is weakened during the evaluation of flexibility.

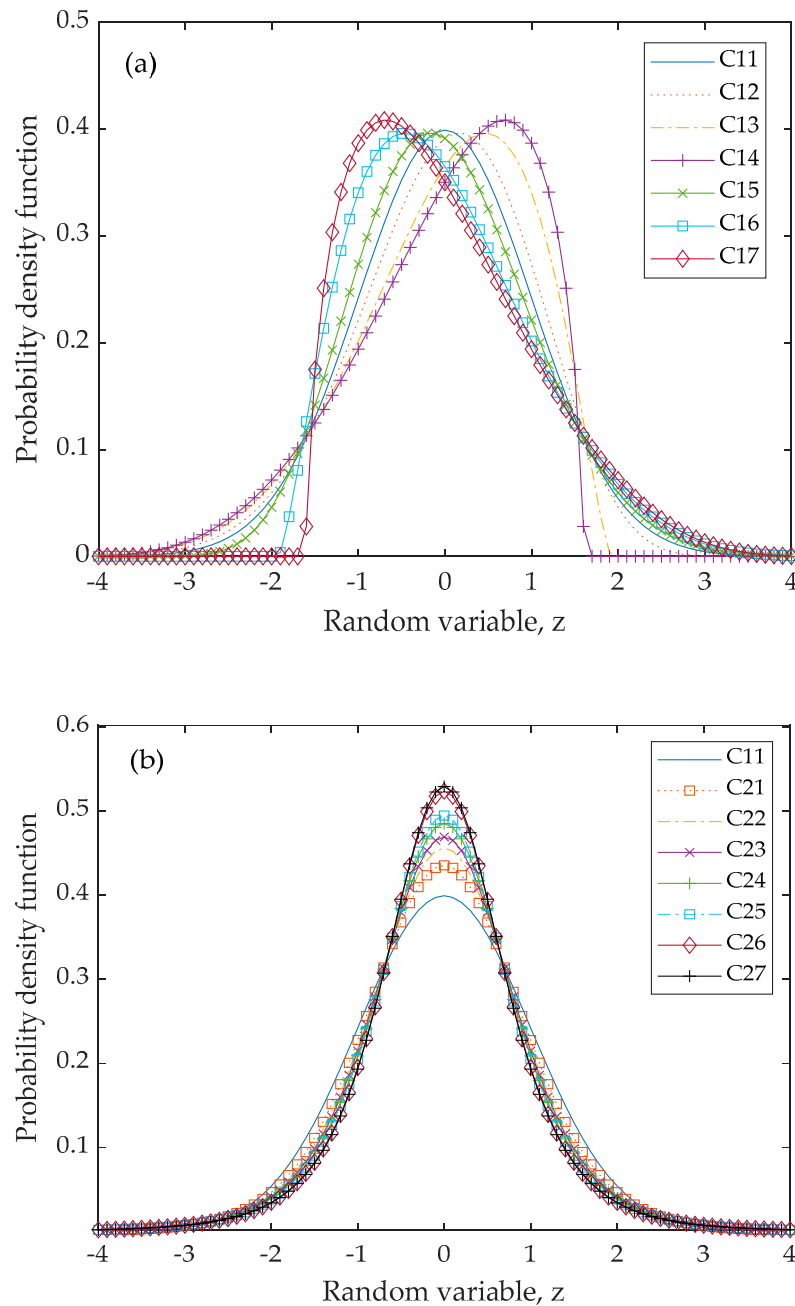


**Figure 2.** Example of Pearson distribution of NLFE: (a) effect of change in skewness, (b) effect of change in kurtosis.

In addition to the NLFE characteristics, the FNL is included as a parameter because it can affect the online state of generating units through the generation schedule and thus the flexibility. The FNL also changes the extent to which the NLFE characteristics affect the flexibility because the NLFE is expressed as the % value of the FNL. Thus, three parameters were considered: skewness, kurtosis, and FNL. The generation schedule and RSP can be varied using these parameters. Its influence on flexibility is the RSP result. The scenarios for NLFE characteristics and FNL are listed in Table 3.

**Table 3.** Scenarios for three parameters: FNL, skewness ( $P_{sk}$ ), kurtosis ( $P_k$ ).

Scenario #	FNL, MW	Skewness, Dimensionless	Kurtosis, Dimensionless
S1	High	Particular range	Fixed
S3		Fixed	Particular range
S4	Medium	Particular range	Fixed
S6		Fixed	Particular range
S7	Low	Particular range	Fixed
S9		Fixed	Particular range

The impact of skewness and kurtosis on flexibility may vary with FNL because the generation schedule can be changed with the FNL. Thus, the FNL is arbitrarily divided into three classes—high, medium, and low. The basic case of the FNL was set to the medium class. The values of skewness and kurtosis are given as a particular range; in particular, the sign of skewness needs to be considered. Each parameter in the scenarios can be selected based on the given system. Empirical approaches can be used to determine the class and level of the FNL. To analyze the individual effect for every FNL, the following condition is considered: the skewness (kurtosis) is fixed, and the kurtosis (skewness) is changed. The influential factor can be determined through the flexibility evaluation for each scenario. The evaluation procedure is summarized in Figure 3.

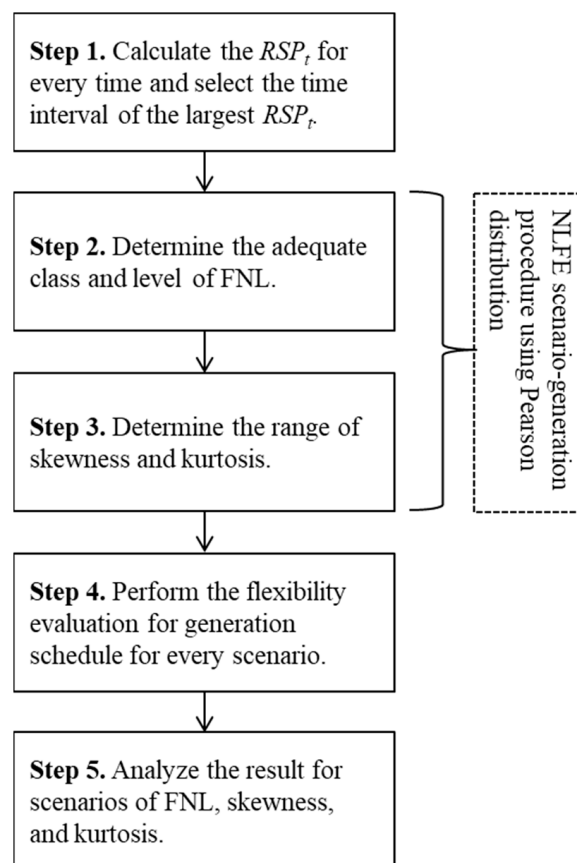


**Figure 3.** Procedure for the effect of NLFE characteristics on flexibility.

#### 4. Case Study

##### Basic Information

The main goal was to investigate the effects of the characteristics of uncertainty on flexibility. A test system is designed by adding the wind power plants of 1250 MW to the IEEE-RTS-96; an effective load-carrying capability of the plants is estimated at

79.88 MW [33]. The test system is composed of 26 generating units of 3,105 MW. Figure 4 shows the FNL profile; a peak load of 2,531 MW occurs at hour 19. The hourly generation schedule is determined using dynamic programming. All generating units are assumed in the spinning state; this condition is required to estimate the maximum value of the flexibility of the system. The  $RSP_t$  was calculated using MATLAB programming (R2020a version) [34]. The simulation for the test system was performed on a PC with 64 GB RAM and a 3.49 GHz CPU. As shown in Figure 5, a seven-step approximation was applied to calculate the probability of the NLFE distribution.

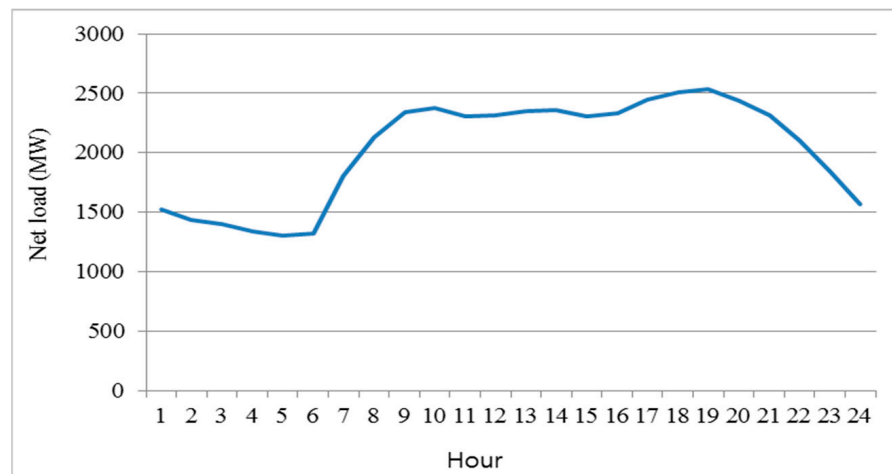


Figure 4. Forecasted net-load profile.

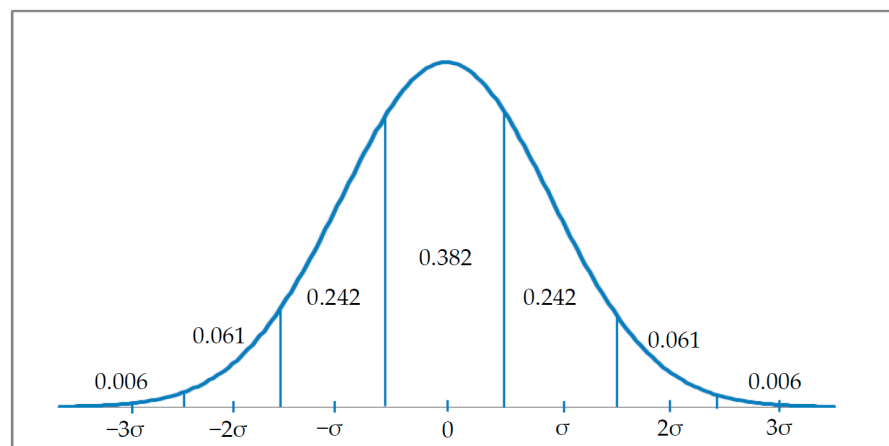


Figure 5.  $NLFE_t$  distribution represented with a seven-step approximation.

According to the solution procedure shown in Figure 3, the following steps were performed. Step 1: The results of the  $RSP_t$  calculation are shown in Figure 6. Hours 18–19 were determined as the most critical time interval because the highest value appears at hour 19.

Steps 2 to 4: Table 4 shows the generated NLFE scenario. The class and level of FNL were selected such that the high class (low class) was set at 101% and 102% (99% and 98%) of the FNL of the base case. A day-ahead NLFE distribution of the California Independent System Operator (CAISO) in the USA is applied as the NLFE of the base case [22]. The values of the mean, standard deviation, skewness, and kurtosis were  $-0.002$ ,  $0.026$ ,  $0.715$ , and  $4.725$ , respectively, and the corresponding PDFs are represented in Figure 7. The standard deviation of the NLFE can be calculated as approximately 65.8 MW, i.e., multiplying 2,531 MW with 0.026 because the “normalized” NLFE (of the x-axis) is

0.026. The ranges of the skewness and kurtosis change from  $-0.115$  to  $1.515$  and  $0.725$  to  $28.725$  with increments of  $0.2$  and  $4$ , respectively. The PDFs for the sampled values of skewness and kurtosis in S5 and S6 are shown in Figure 8.

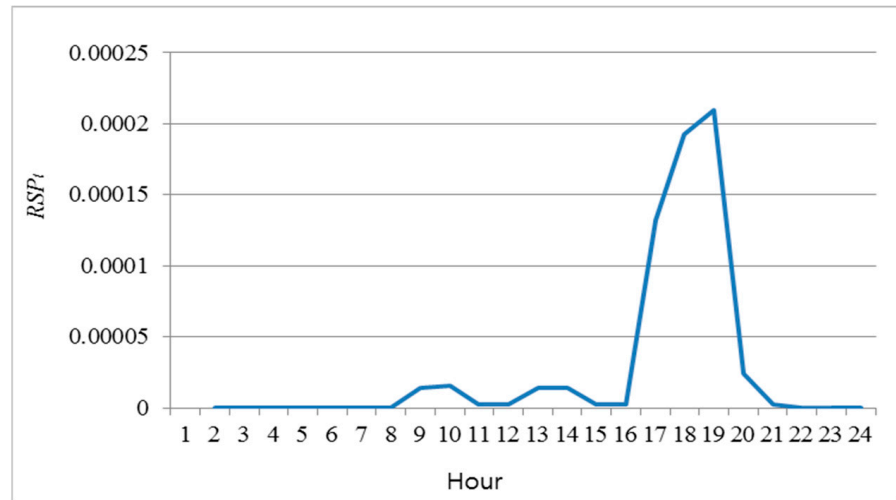


Figure 6. Hourly  $RSP_t$ .

Table 4. Scenario for three parameters: FNL, skewness ( $P_{sk}$ ), kurtosis ( $P_k$ ).

Scenario, S#	FNL, %	Skewness, Dimensionless	Kurtosis, Dimensionless
S1	102%	$-0.115$ to $1.515$	Fixed, i.e., $4.725$
S2	102%	Fixed, i.e., $0.715$	$0.725$ to $28.725$
S3	101%	$-0.115$ to $1.515$	Fixed, i.e., $4.725$
S4	101%	Fixed, i.e., $0.715$	$0.725$ to $28.725$
S5	100%	$-0.115$ to $1.515$	Fixed, i.e., $4.725$
S6	100%	Fixed, i.e., $0.715$	$0.725$ to $28.725$
S7	99%	$-0.115$ to $1.515$	Fixed, i.e., $4.725$
S8	99%	Fixed, i.e., $0.715$	$0.725$ to $28.725$
S9	98%	$-0.115$ to $1.515$	Fixed, i.e., $4.725$
S10	98%	Fixed, i.e., $0.715$	$0.725$ to $28.725$

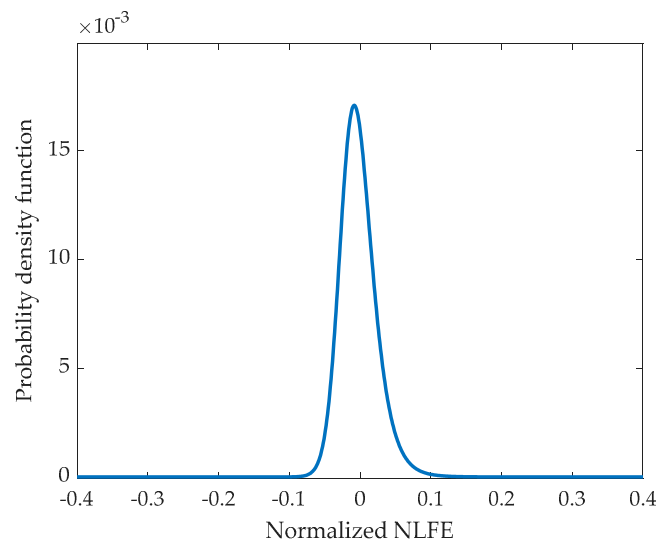
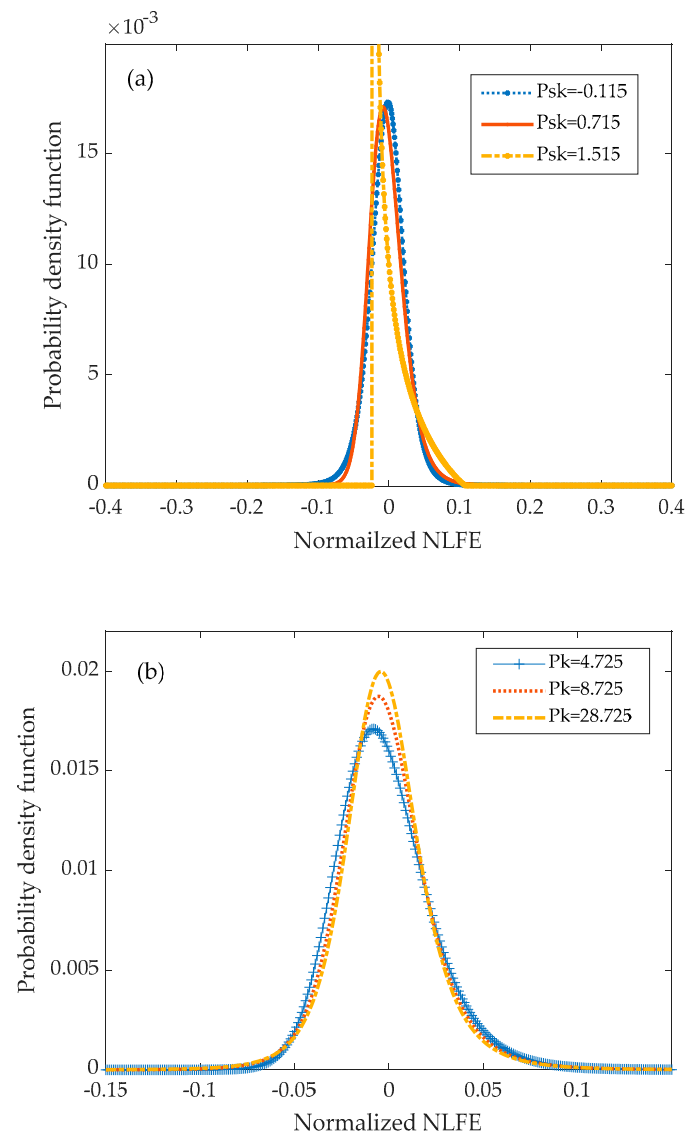


Figure 7. Probability density function of normalized NLFE.



**Figure 8.** Probability density function of normalized NLFE: (a) result of changes in skewness in S5, (b) result of changes in kurtosis in S6.

Step 5: The hourly generation schedules for every scenario, i.e., S1 to S10, are determined based on the given FNL. Flexibility evaluation was later performed for every scenario. Figures 9 and 10 show the  $RSP_t$  results according to the changes in skewness and kurtosis over a certain range, respectively. In both Figures,  $RSP_t$  decreases (increases) according to the decrease (increase) in the FNL. This is because the available reserve capacity of the generating unit varies with the FNL.

In each Figure, a sudden change in  $RSP_t$  occurs, i.e., the points of change lie between S5 and S7, and S6 and S8 in Figures 9 and 10, respectively. Sensitivity analysis was performed for both skewness- and kurtosis-varying scenarios; the points of change were 99.7% of the FNL of the base case in both scenarios. If the  $RSP_t$  is evaluated for a wider range of FNL than that of the FNL of the scenario, more points of change may appear. The changes in the FNL can cause a sudden change in the  $RSP_t$  because the committed set and operating conditions of the generating units change before and after the point of change. When there is no abrupt change in the  $RSP_t$ , the changes in skewness and kurtosis were more influential than the FNL. It can be simply confirmed by comparing S7 and S9 that the  $RSP_t$  in both scenarios increases with skewness; however, there is little difference between  $RSP_t$  in these scenarios as the skewness changes.

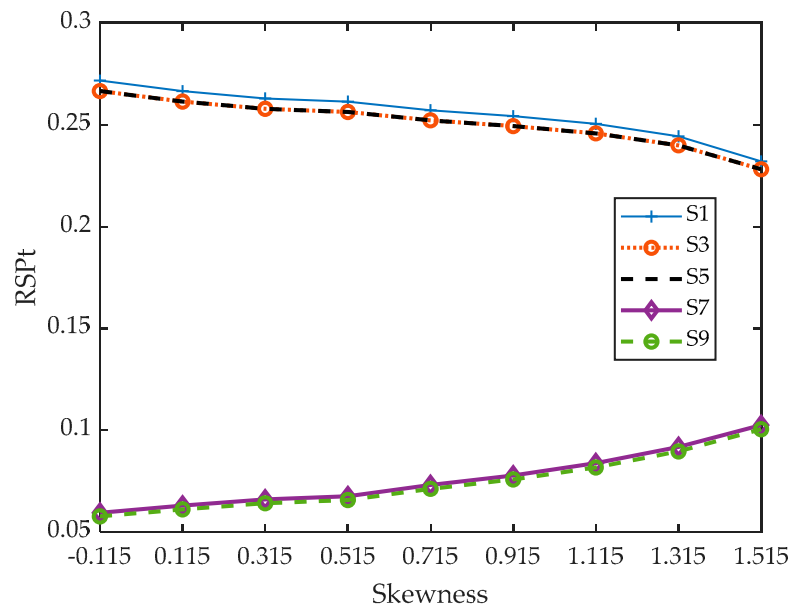


Figure 9.  $RSP_t$  results for skewness-varying scenarios, i.e., S1, S3, S5, S7, and S9.

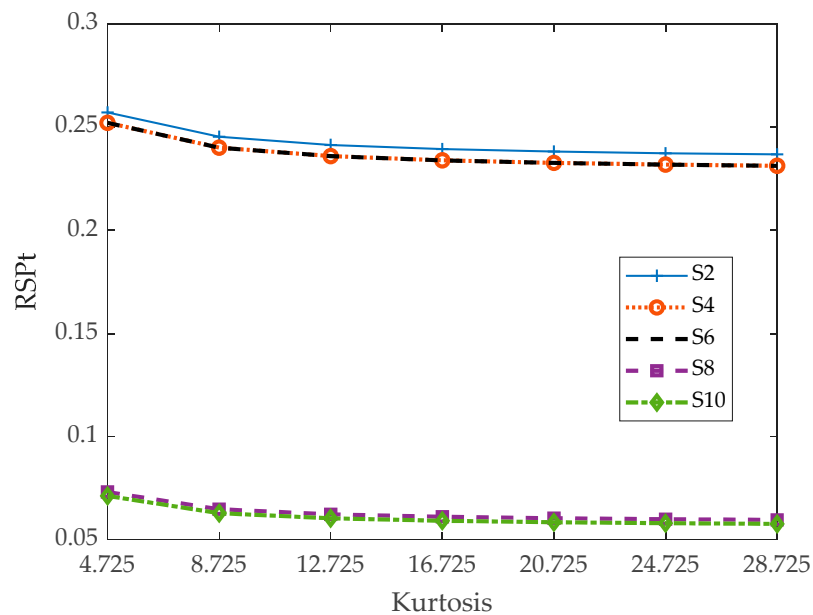


Figure 10.  $RSP_t$  results for kurtosis-varying scenarios, i.e., S2, S4, S6, S8, and S10.

The ratio of the skewness increment, i.e., 0.2 (the kurtosis increment, i.e., 4), to the skewness (kurtosis) of the base case is approximately 28% (85%). The ratio for skewness is smaller than that for kurtosis; however, the effect of skewness is greater than that of kurtosis. It can be compared with the relative  $RSP_t$  ratio, defined as the  $RSP_t$  divided by the ratio calculated above. The largest relative  $RSP_t$  for the skewness-varying (kurtosis-varying) scenario is 4.19% (1.41%); for reference, the largest changes in  $RSP_t$  in the skewness-varying and kurtosis-varying scenarios are between 4.725 and 8.725 and 1.315 and 1.515 in S5 and S6, respectively. The average value of the relative  $RSP_t$  for the skewness-varying (kurtosis-varying) scenarios for the entire interval was 1.72% (0.41%). In the kurtosis-varying scenarios, the  $RSP_t$  in S2, S4, S6, S8, and S10 decreases with an increase in kurtosis. In the skewness-varying scenarios, the  $RSP_t$  in S7 and S9 increases with an increase in skewness, whereas those in S1, S3, and S5 decrease. If the PDF is skewed to the left (i.e., the increase in skewness), it indicates that the load unexpectedly decreases. The  $RSP$

index captures the risk associated with increasing loads only; thus, decreasing loads can be considered better cases in terms of risk, and therefore, the  $RSP_t$  (i.e., risk) decreases. This is because the probability of small normalized NLFEs is also reduced. This is confirmed by the graphs in Figure 8a.

## 5. Conclusions

This study investigated the impact of skewness and kurtosis of the NLFE on flexibility. The contribution is to propose a method for the effective analysis of NLFE characteristics on flexibility. The effect on flexibility was captured using a flexibility index called RSP. The skewness and kurtosis of the NLFE were represented with a Pearson distribution. A case study for a modified IEEE-RTS-96 was conducted for the scenarios of FNL, skewness, and kurtosis. The simulation results also indicated that an abrupt change in the RSP can occur with the increase in the FNL. It was also observed that skewness with fixed kurtosis was more effective than kurtosis with fixed skewness. The proposed method is expected to help system operators to cope with changes in uncertainty characteristics. In future work, the application of this method to a real power system will be interesting.

**Funding:** This research was funded by the Joongbu University Research and Development Fund in 2019.

**Institutional Review Board Statement:** Not applicable.

**Informed Consent Statement:** Not applicable.

**Conflicts of Interest:** The author declares no conflict of interest.

## References

1. International Renewable Energy Agency. *Global Energy Transformation: A Roadmap to 2050*; IRENA: Abu Dhabi, United Arab Emirates, 2018.
2. The Ministry of Trade, Industry and Energy. *Energy Transformation Roadmap in Korea*; MOTIE: Sejong, Korea, 2017.
3. The Ministry of Trade, Industry and Energy. *Renewable Energy 3020 Implementation Plan*; MOTIE: Sejong, Korea, 2017.
4. The Ministry of Trade, Industry and Energy. *The 9th Basic Plan on Electricity Demand and Supply*; MOTIE: Sejong, Korea, 2020.
5. The Ministry of Trade, Industry and Energy. *5th Renewable Energy Basic Plan*; MOTIE: Sejong, Korea, 2020.
6. Wu, Q.; Hu, Q.; Hang, L.; Botterud, A.; Muljadi, E. Power to Gas for Future Renewable based Energy Systems. *IET Renew. Power Gener.* **2021**, *14*, 3281–3283.
7. Min, C.-G. Analyzing the impact of variability and uncertainty on power system flexibility. *Appl. Sci.* **2019**, *9*, 561. [[CrossRef](#)]
8. Mohandes, B.; El Moursi, M.S.; Hatziargyriou, N.; El Khatib, S. A review of power system flexibility with high penetration of renewables. *IEEE Trans. Power Syst.* **2019**, *34*, 3140–3155. [[CrossRef](#)]
9. Babatunde, O.; Munda, J.; Hamam, Y. Power system flexibility: A review. *Energy Rep.* **2020**, *6*, 101–106. [[CrossRef](#)]
10. Cochran, J.; Miller, M.; Zinaman, O.; Milligan, M.; Arent, D.; Palmintier, B.; O'Malley, M.; Mueller, S.; Lannoye, E.; Tuohy, A. *Flexibility in 21st Century Power Systems*; National Renewable Energy Laboratory (NREL): Golden, CO, USA, 2014.
11. Zhao, J.; Zheng, T.; Litvinov, E. A unified framework for defining and measuring flexibility in power system. *IEEE Trans. Power Syst.* **2015**, *31*, 339–347. [[CrossRef](#)]
12. Degefa, M.Z.; Sperstad, I.B.; Sæle, H. Comprehensive classifications and characterizations of power system flexibility resources. *Electr. Power Syst. Res.* **2021**, *194*, 107022. [[CrossRef](#)]
13. Lin, H.; Wang, C.; Wen, F.; Tseng, C.-L.; Hu, J.; Ma, L.; Fan, M. Risk-Limiting Real-Time Economic Dispatch in a Power System with Flexibility Resources. *Energies* **2019**, *12*, 3133. [[CrossRef](#)]
14. Pappala, V.S.; Erlich, I.; Rohrig, K.; Dobschinski, J. A stochastic model for the optimal operation of a wind-thermal power system. *IEEE Trans. Power Syst.* **2009**, *24*, 940–950. [[CrossRef](#)]
15. Cong, P.; Tang, W.; Zhang, L.; Zhang, B.; Cai, Y. Day-ahead active power scheduling in active distribution network considering renewable energy generation forecast errors. *Energies* **2017**, *10*, 1291. [[CrossRef](#)]
16. Yu, X.; Dong, X.; Pang, S.; Zhou, L.; Zang, H. Energy storage sizing optimization and sensitivity analysis based on wind power forecast error compensation. *Energies* **2019**, *12*, 4755. [[CrossRef](#)]
17. García-Bustamante, E.; González-Rouco, J.; Jiménez, P.; Navarro, J.; Montávez, J. The influence of the Weibull assumption in monthly wind energy estimation. *Wind Energy Int. J. Prog. Appl. Wind Power Convers. Technol.* **2008**, *11*, 483–502. [[CrossRef](#)]
18. Ellahi, M.; Abbas, G.; Khan, I.; Koola, P.M.; Nasir, M.; Raza, A.; Farooq, U. Recent approaches of forecasting and optimal economic dispatch to overcome intermittency of wind and photovoltaic (PV) systems: A review. *Energies* **2019**, *12*, 4392. [[CrossRef](#)]
19. Bludszuweit, H.; Domínguez-Navarro, J.A.; Llombart, A. Statistical analysis of wind power forecast error. *IEEE Trans. Power Syst.* **2008**, *23*, 983–991. [[CrossRef](#)]

20. Lange, M. On the uncertainty of wind power predictions—Analysis of the forecast accuracy and statistical distribution of errors. *J. Sol. Energy Eng.* **2005**, *127*, 177–184. [[CrossRef](#)]
21. Goodarzi, S.; Perera, H.N.; Bunn, D. The impact of renewable energy forecast errors on imbalance volumes and electricity spot prices. *Energy Policy* **2019**, *134*, 110827. [[CrossRef](#)]
22. Hodge, B.-M.; Florita, A.; Orwig, K.; Lew, D.; Milligan, M. *Comparison of Wind Power and Load Forecasting Error Distributions*; National Renewable Energy Laboratory (NREL): Golden, CO, USA, 2012.
23. Khoshjahan, M.; Dehghanian, P.; Moeini-Aghaie, M.; Fotuhi-Firuzabad, M. Harnessing ramp capability of spinning reserve services for enhanced power grid flexibility. *IEEE Trans. Ind. Appl.* **2019**, *55*, 7103–7112. [[CrossRef](#)]
24. Eni, R.O.; Akinbami, J.-F.K. Flexibility evaluation of integrating solar power into the Nigerian electricity grid. *IET Renew. Power Gener.* **2016**, *11*, 239–247. [[CrossRef](#)]
25. Lu, Z.; Li, H.; Qiao, Y. Probabilistic flexibility evaluation for power system planning considering its association with renewable power curtailment. *IEEE Trans. Power Syst.* **2018**, *33*, 3285–3295. [[CrossRef](#)]
26. Min, C.; Park, J.; Hur, D.; Kim, M. A risk evaluation method for ramping capability shortage in power systems. *Energy* **2016**, *113*, 1316–1324. [[CrossRef](#)]
27. Allan, R.N. *Reliability Evaluation of Power Systems*; Springer Science & Business Media: Berlin, Germany, 2013.
28. Min, C.-G.; Kim, M.-K. Flexibility-based reserve scheduling of pumped hydroelectric energy storage in Korea. *Energies* **2017**, *10*, 1478.
29. Min, C.-G.; Kim, M.-K. Flexibility-based evaluation of variable generation acceptability in Korean power system. *Energies* **2017**, *10*, 825. [[CrossRef](#)]
30. Rajbhandari, N.; Li, W.; Du, P.; Sharma, S.; Blevins, B. Analysis of net-load forecast error and new methodology to determine non-spin reserve service requirement. In Proceedings of the 2016 IEEE Power and Energy Society General Meeting (PESGM), Boston, MA, USA, 17–21 July 2016; pp. 1–5.
31. Tayebi, N.; Polycarpou, A.A. Modeling the effect of skewness and kurtosis on the static friction coefficient of rough surfaces. *Tribol. Int.* **2004**, *37*, 491–505. [[CrossRef](#)]
32. Kotwal, C.A.; Bhushan, B. Contact analysis of non-Gaussian surfaces for minimum static and kinetic friction and wear. *Tribol. Trans.* **1996**, *39*, 890–898. [[CrossRef](#)]
33. Milligan, M.; Porter, K. *Determining the Capacity Value of Wind: An Updated Survey of Methods and Implementation*; National Renewable Energy Laboratory (NREL): Golden, CO, USA, 2008.
34. Hunt, B.R.; Lipsman, R.L.; Rosenberg, J.M. *A Guide to Matlab: For Beginners and Experienced Users*; Cambridge University Press: Cambridge, UK, 2014.